

copy 3.
BMR PUBLICATIONS COMPACTUS
(LENDING SECTION)



DEPARTMENT OF
NATIONAL RESOURCES

BUREAU OF MINERAL RESOURCES,
GEOLOGY AND GEOPHYSICS

Record 1977/39

055802⁺

MEASUREMENTS OF SURFACE HEAT FLOW



by.

J.P. CULL AND G.F. SPARKSMAN

The information contained in this report has been obtained by the Department of National Resources as part of the policy of the Australian Government to assist in the exploration and development of mineral resources. It may not be published in any form or used in a company prospectus or statement without the permission in writing of the Director, Bureau of Mineral Resources, Geology and Geophysics.

BMR
Record
1977/39
c.3

Record 1977/39

MEASUREMENTS OF SURFACE HEAT FLOW

by

J.P. CULL AND G.F. SPARKSMAN

CONTENTS

	<u>Page Nos.</u>
ABSTRACT	1
1. INTRODUCTION	2
2. TEMPERATURE GRADIENTS	2
3. THERMAL CONDUCTIVITIES	8
4. CALCULATIONS OF HEAT FLOW	13
5. ACKNOWLEDGEMENTS	15
6. REFERENCES	15

TABLE

1. Critical thermal gradients required to cause convection in vertical cylinders containing water.

FIGURES

1. Schematic for eliminating lead resistance in Wheatstone Bridge circuit used with a down-hole thermistor probe
2. Secular perturbation of temperature gradient (step function of 5°C at surface).
3. Principal components in divided-bar thermal-conductivity apparatus.
4. Heat flux in principal segments of divided-bar sample stack.
5. Determination of contact resistance in divided-bar stack segments.
6. Cell designed to contain core fragments in divided-bar apparatus.
7. Comparison of conductivity values determined using (1) solid core and (2) fragments.
8. Mean annual air temperature as a function of latitude.
9. Temperature/depth profile for borehole CAN 145. Determinations of heat flow from linear segments.
10. Bullard reduction of data presented in Fig. 9. Determination of heat flow.

ABSTRACT

Heat flow studies are now included in programs conducted by BMR. Thermal gradients are measured (with resolution of 0.001°C) at depths greater than 100 m; they are considered to be free from climatic perturbations except in regions affected by Quaternary glaciation. Convection in observation bores or in permeable sedimentary strata is considered unlikely.

Thermal conductivities are determined using a divided-bar apparatus; side losses and contact resistance are included in the reduction. It is estimated for solid core that thermal conductivities can be measured with an accuracy of $\pm 2\%$. However, the cell technique (used in measuring the conductivity of fragments) can lead to errors of $+20\%$ and calibration may be necessary.

Geothermal data are reported for a borehole in the Canberra 250 000 Sheet area; reduction techniques are demonstrated and a value 72.9 mW m^{-2} is obtained for the heat flow in that region.

1. INTRODUCTION

A detailed knowledge of the temperature field in the Earth's crust and mantle is fundamental to the formulation of tectonic and geochemical models. Temperature data are also required for the particular purpose of locating geothermal energy prospects. Additionally, for petroleum prospects, the thermal history of a region may be crucial in estimating levels of maturation. In each case, observations of surface heat flow are required so that surface temperatures can be extrapolated at depth.

Surface heat flow Q (W.m^{-2}) is calculated from the expression

$$Q = \lambda \beta \quad (1)$$

where β (K.m^{-1}) is the thermal gradient in any location, and λ ($\text{W.m}^{-1}.\text{K}^{-1}$) is the thermal conductivity of the rocks in which the gradient is established.

It is the purpose of this paper to discuss the techniques commonly used to measure λ and β . Limits of error are proposed and limitations are considered for techniques used within the Bureau of Mineral Resources (BMR). Heat flow data are reported for a borehole in Canberra to demonstrate methods of reduction.

2. TEMPERATURE GRADIENTS

On land, temperature gradients must be determined at depths in excess of 100 m so that climatic perturbations (discussed below) can be avoided. Consequently the temperature sensing device must be attached to a long cable which can be lowered to successively greater depths. Originally, maximum-reading mercury thermometers were used for this purpose; however, multiple runs are required to obtain data from different depths and the accuracy is generally less than 0.1°C . Electronic devices offer the advantages of increased accuracy, continuous profiling, and speed of operation.

Differential thermocouples, variable frequency devices, and temperature-sensitive resistors (thermistors or platinum wire) are the most common electronic thermometers. Of these the thermistor sensor is the most attractive; it is sensitive, inexpensive, and does not require massive cables or complicated electronics. In the BMR system a Fenwal thermistor (type UUA33J1, nom. 3K at 25°C) is attached to the end of the cable (geophone leader, 4 core, total O.D. 4.2 mm, breaking strength 100 kg) according to Figure 1. A Wheatstone bridge, used to monitor the resistance of the sensor, has the capability of resolving changes of 0.2 ohms (representing temperature changes of the order of 0.001°C). Before the thermistor probe can be used, however, it must be calibrated against a standard platinum thermometer. Calibration errors and subsequent thermistor drift can contribute uncertainties of 0.01°C in absolute readings of temperature but, for determinations of thermal gradient, only the relative values are important.

Climatic effects

Heat generated within the Earth escapes by conduction at rates of the order of 100 mW.m⁻². In contrast, heat is received from the Sun by radiation at rates up to 1000 W.m⁻². Temperatures measured close to the Earth's surface will then obviously depend on climatic variations. Geothermal gradients must be measured at depths which are not affected by the propagation of such perturbations.

Seasonal and diurnal changes in solar heating are the most obvious source of periodic fluctuations in surface temperature. Carslaw & Jaeger (1959, p#65) have considered the problem of periodic surface heating and they derive the solution

$$T = T_0 \exp(-\epsilon z) \cos(\omega t - \epsilon z) \quad (2)$$

where $\omega = 2\pi/P$, P is the period, $\epsilon = (\omega/2K)^{1/2}$, and K is the thermal diffusivity.

The time-dependent term results in an effective wavelength $(4\pi K P)^{1/2}$ approximately equal to 1 metre for the diurnal wave and 20 metres for the annual wave (assuming a representative $K = 10^{-6} \text{ m}^2/\text{s}$). The maximum amplitude of the disturbance is governed by the exponential term in equation

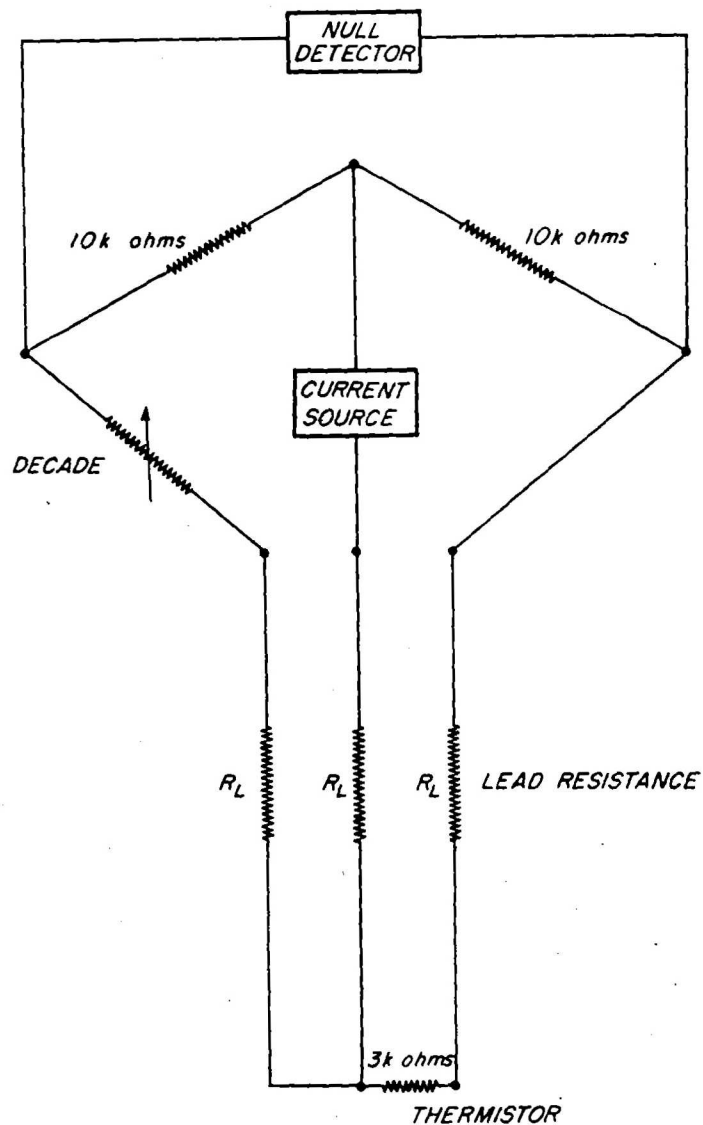


Fig.1 Schematic for eliminating lead resistance in Wheatstone bridge circuit used with a down-hole thermistor probe.

(2). At a depth of one wavelength the surface amplitude is reduced by a factor $\exp(-2\pi) = 0.0019$, and consequently for most purposes it can be considered that the disturbance at greater depths is negligible.

Secular changes in climate are not well determined. Short-term (< 10 year) trends can be discerned from available data (Tucker, 1975) but deviations are usually within 1°C of mean values. It is well established that there was a period of glaciation in Tasmania and in the Snowy Mountains region, but the extent and duration are not well defined. However, it is generally considered that this period ceased 10-20 thousand years B.P. and that temperatures subsequently increased by $5-10^{\circ}\text{C}$. Geothermal gradients measured at the present time in these regions may still be perturbed by this sudden increase in surface temperature.

The effect of a simple temperature step function (5°C) is shown in Figure 2. After a period of 10 000 years there is only slight curvature; this may not be detected in borehole data, and the apparent gradient may be in error by 20%. At depths greater than 1000 m the error reduces to less than 5%.

In practice, temperatures are obtained in boreholes at depths greater than 100 m (and commonly 300 m). These depths are great enough to allow the periodic effects to be neglected; moreover, at these depths there are no uncertainties concerning water-table movements or conductivity variations due to weathering. Corrections must be applied, however, in those regions which have been subject to glaciation.

Thermal equilibrium

To obtain temperatures at depths greater than 100 m it is first necessary to drill suitable boreholes. Unfortunately the process of drilling disturbs the established temperature gradient. There are two sources of disturbance:

- (1) friction at the cutting face, and
- (2) circulation of drilling fluids through the bore from the surface.

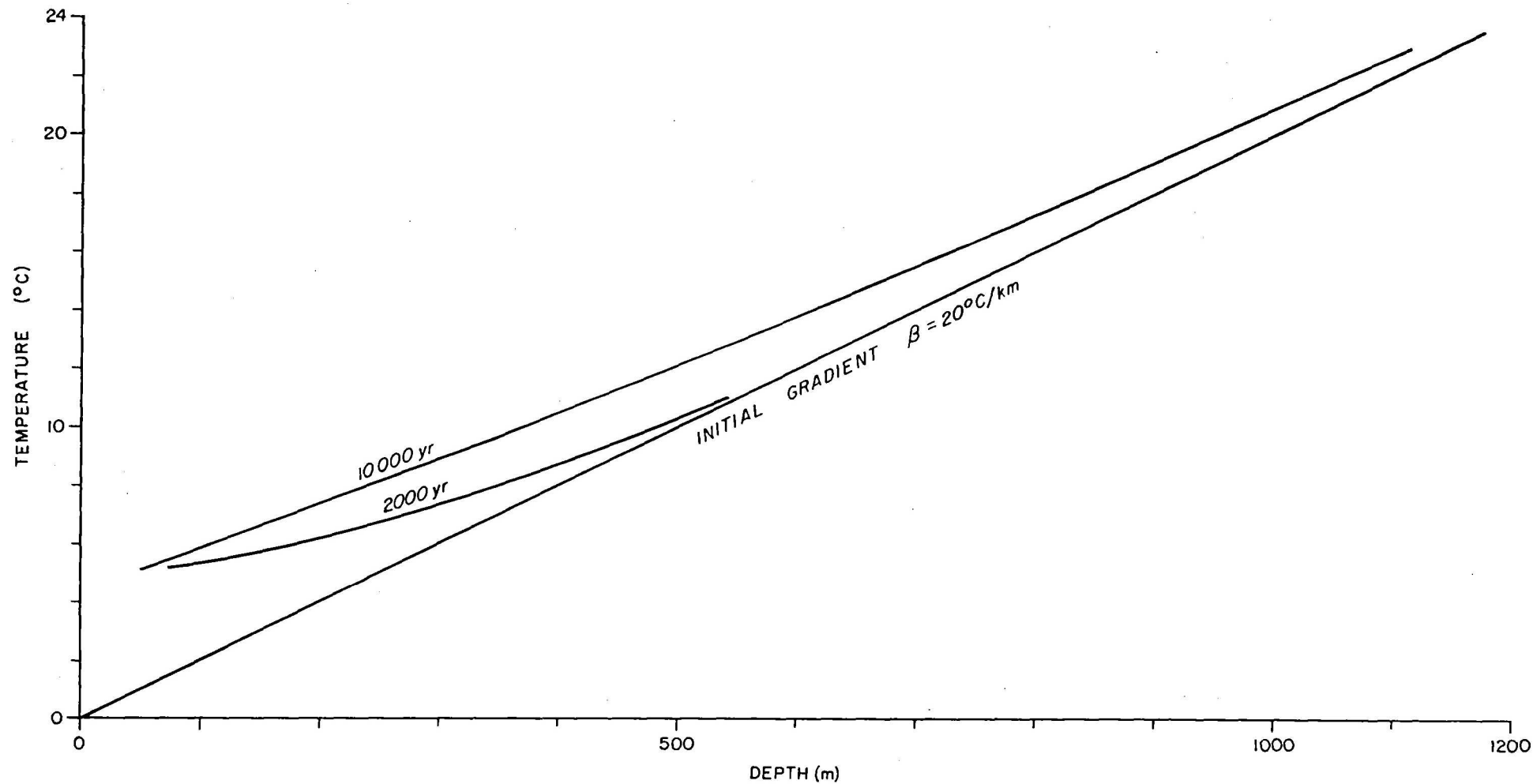


Fig.2 Secular perturbation of temperature gradient (step function of 5°C at surface).

At any given depth heat is generated by friction only for a very short time as the cutting face moves progressively deeper. In contrast, mud is usually circulated through the hole for the full duration of drilling. Heat may be conducted away from (or towards) the bore for periods in excess of one week (typically four weeks for a 300 m bore). Gradients measured at the completion of drilling consequently have little meaning.

By assuming that drilling disturbances can be approximated by a line source of heat, Bullard (1947) calculated the times necessary to regain equilibrium. He demonstrated that measured temperatures will be correct to 1% after a time lapse equivalent to ten times the duration of drilling. In studies conducted by BMR, thermal gradients are usually determined at depths between 100 m and 300 m; a minimum of twelve months is allowed for equilibration.

In many holes there is danger of caving during the period of equilibration and consequently casing must be inserted. PVC pressure pipe (3.5 cm diam.) is adequate for this purpose; it can be easily transported, it is rapidly joined with solvent glues, and it is inexpensive (\$1 per metre).

Temperatures measured in such cased holes do not exactly reflect conditions in the surrounding rock even if equilibrium is fully restored. The isotherms are refracted by variations in thermal conductivity at the bore/casing interface. For PVC casing, heat is conducted more slowly than in the surrounding rock; temperatures are restored to equilibrium by a complex horizontal component of heat flow. In practice it is not possible to use observations in cased boreholes to detect changes in thermal gradient caused by the presence of thin strata (i.e. less than 50 cm approx.).

Borehole convection

If convection occurs within the borehole, measured temperatures may not be locally related to thermal gradients in the surrounding rock. Convection occurs when a fluid is heated from below; thermal expansion causes a density inversion and a flow results when gravitational forces are greater than the internal friction (i.e. viscosity) of the liquid and the friction of contact with the walls of the container. For liquids contained in vertical cylinders, Hales (1937) derived the expression

$$\beta_c = \frac{g \alpha T}{C_p} + \frac{216 \nu \chi}{g \alpha a^4} \quad (3)$$

where β_c is the critical (minimum) thermal gradient required to cause convection, ν is the kinematic viscosity, χ is the thermal diffusivity, C_p is the specific heat, and α is the coefficient of thermal expansion of the liquid. The symbol a refers to the radius of the cylinder, g is the gravitational constant and T is absolute temperature.

Hales's expression has been confirmed experimentally by Auld (1948) and observations have been made in deep boreholes by Krige (1939), Diment (1967), and Gretener (1967). Temperature fluctuations are rarely detected even when instabilities are predicted from the theory (Table 1). Vertical movements must therefore be very small and any flow is confined to cells with height about equal to the borehole diameter. Oscillations would then occur with an amplitude less than 0.05°C (Diment, 1967).

Geothermal gradients rarely exceed $50^\circ\text{C}/\text{km}$ and more commonly they are close to $25^\circ\text{C}/\text{km}$. Consequently it can be seen from Table 1 that borehole convection need be considered only when casing diameters exceed 4 cm. Temperatures measured within convecting intervals will reflect the critical gradient, and determinations of heat flow may be impossible.

TABLE 1.

Critical thermal gradients required to cause convection in vertical cylinders containing water (calculated from equation 3).

Temp. ($^\circ\text{C}$)	Fluid parameters			Critical gradient β_c ($^\circ\text{C}/\text{km}$)		
	α (K^{-1})	χ (m^2/s)	ν (m^2/s)	cylinder radius (cm)		
				$a = 1$	$a = 2$	$a = 3$
25	2.6×10^{-4}	1.49×10^{-7}	8.9×10^{-7}	1120	70	15
50	4.5	1.56	5.6	430	27	6
75	6.0	1.64	3.9	230	14	3
100	7.0	1.71	2.9	156	10	2

Symbols

- α coefficient of thermal expansion
- κ thermal diffusivity
- ν kinematic viscosity
- a cylinder radius
- β_c critical thermal gradient

Groundwater convection

For determinations of heat flow it is essential that measurements be made in a wholly conductive regime. If there is a flow of water across an observation bore, the vertical component of flow must be considered as a mode of heat transfer. Usually it is impossible to make an accurate estimate of the quantity of heat transferred in this manner.

In sedimentary basins deep aquifers are common; slow migrations of water do occur but the component of flow is mostly horizontal. However, the possibility does exist for local convective cells to be established in these aquifers. Horton & Rogers (1945) first examined the problem of convection in porous media; they derived the expression

$$\beta_c = \frac{4\pi^2 \kappa_m \nu}{f g \alpha D^2} \quad (4)$$

where D is the thickness of the sequence, f is the permeability, and κ_m is the thermal diffusivity. The other parameters are as described above.

This expression was confirmed by Lapwood (1948) and demonstrated experimentally by Elder (1965).

The permeability of sandstones is highly variable, ranging between 10^{-7} and 10^{-4} m^2 (values as large as 10^{-2} m^2 may be obtained for silts). In high-yield aquifers, a figure of 10^{-4} m^2 may not be unreasonable. With this and other representative values in equation (4) the critical gradient can be expressed as

$$\beta_c = 10^2 / D^2 \quad (5)$$

If D is of the order of 10 m, then the critical gradient calculated from equation (5) is 1000°C/km .

Except for hydrothermal regions, geothermal gradients seldom exceed 50°C/km and consequently convection within basin aquifers is considered unlikely.

3. THERMAL CONDUCTIVITIES

For determinations of heat flow it is necessary to know both the thermal gradient and the thermal conductivity of the rocks in which the gradient is established (equation 1). The technique used in measuring thermal conductivity depends upon the type of core available. If the core is well consolidated, small samples of regular geometry can be machined and steady temperature fields can be established. However, for muds and friable core, machining is impossible and transient techniques must be used. At present, steady-state techniques are considered the most accurate; they are preferred for this reason even though sample preparation is laborious.

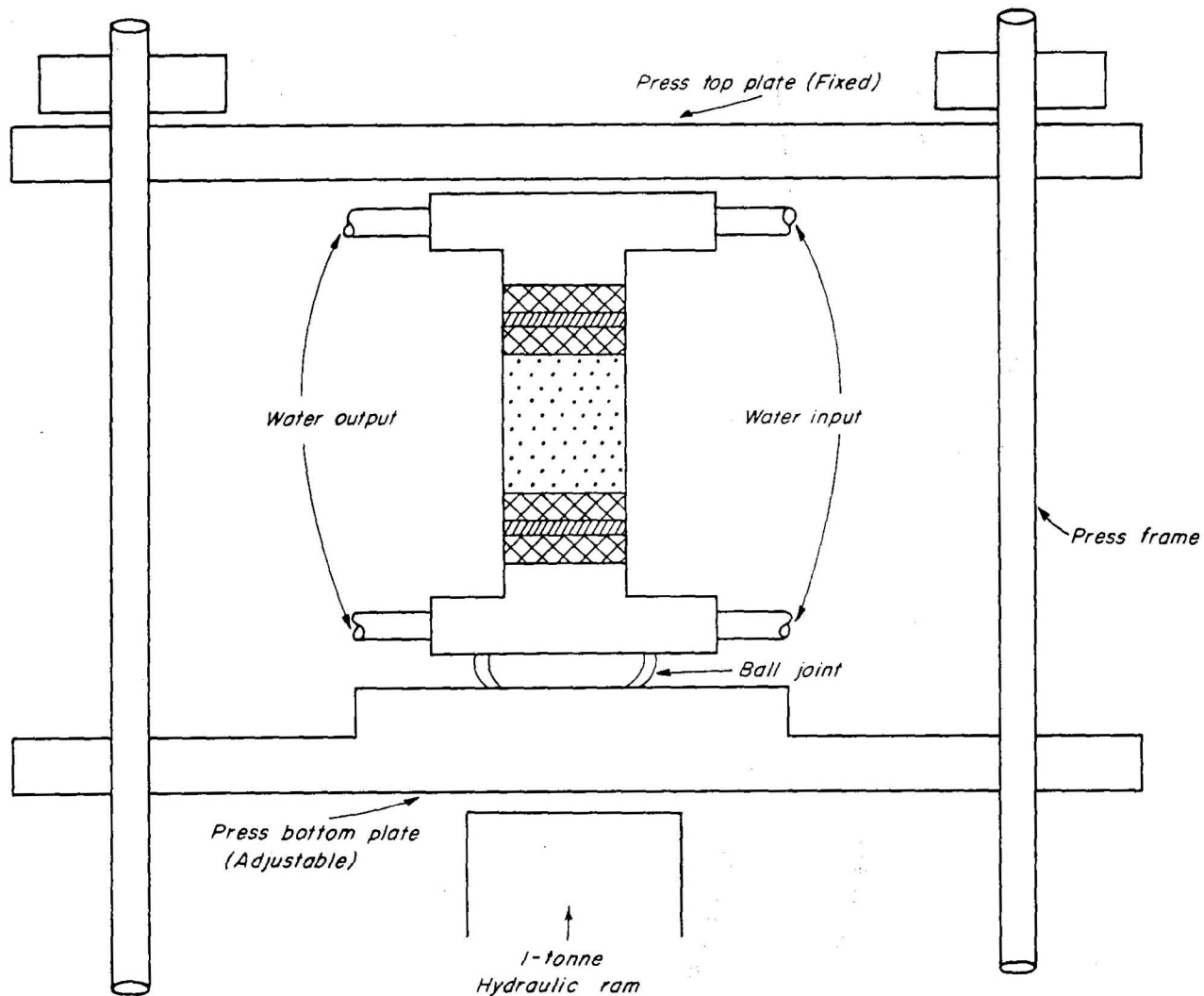
DIVIDED-BAR APPARATUS

Of the steady-state techniques the divided bar is by far the most common. There are several configurations but for geophysical work the system described by Birch (1950) is the most suitable (see also Beck 1957; Sass et al., 1971a). Cylindrical samples must first be cored; their end faces are then ground flat and they are stacked axially with a standard material between the faces of a vertical press (Fig. 3). A steady flow of heat is established through the stack by maintaining different temperatures at the top and bottom faces of the press (the top face is kept hotter than the bottom face to avoid possible convection in water-saturated samples).

If it is assumed that the heat flux is constant through the stack then the conductivity of the sample (suffix S) is found (in accord with equation 1) from the expression

$$\lambda_s = \lambda_R \beta_R / \beta_s \quad (6)$$

Discs of silica glass or of quartz can be used as the reference material (suffix R) but secondary standards may be calibrated for routine operation.






- | | |
|---|---|
|  | Lexan (heat flux comparators) |
|  | Brass discs (containing chromel/alumel thermocouples) |
|  | Sample under test |

Fig.3 Principal components in divided-bar thermal-conductivity apparatus

In the BMR apparatus two secondary standards of LEXAN, a polycarbonate, are used at each end of the stack to allow two separate determinations of the heat flux. A guard ring is not included but radial loss of heat is reduced by insulating with polystyrene foam. Temperatures in the stack are monitored with chromel/alumel thermocouples switched to a 4½ digit nanovoltmeter (Keithley, model 180). Relative temperatures can be determined to an accuracy of 0.002°C.

Calibration

Ratcliffe's (1959) values for the thermal conductivity of quartz are used for calibrating the secondary standards. If no heat is lost from the sides of the stack, calibration is simple. Heat flux is constant through the stack and consequently the thermal gradients are directly related to the conductivity of each segment. A core of quartz crystal (Qtz) can be placed in the sample space and (consistent with equation 6) the conductivity of the LEXAN (L) can be determined from the expression.

$$\lambda L = \lambda_{Qtz} \beta_{Qtz} / \beta_L$$

It is found in practice, however, that side losses of heat are significant (particularly in apparatus where there are no guard rings). Equation (6) is therefore not generally applicable since heat flux decreases continuously through the stack. Referring to Figure 4 the heat flux in the three segments can be related by the expressions

$$Q_M = Q_T - f Q_L \quad (7a)$$

$$Q_M = Q_B + (1 - f) Q_L \quad (7b)$$

where Q_T is the heat flux through the top standard

Q_M is the average heat flux through the sample space

Q_B is the heat flux through the bottom standard

Q_L is the total radial heat loss

and f is the fraction of Q_L lost in the top half of the stack.

Eliminating Q_L , these equations can be reduced to give

$$Q_T = Q_M + f (Q_T - Q_B) \quad (8)$$

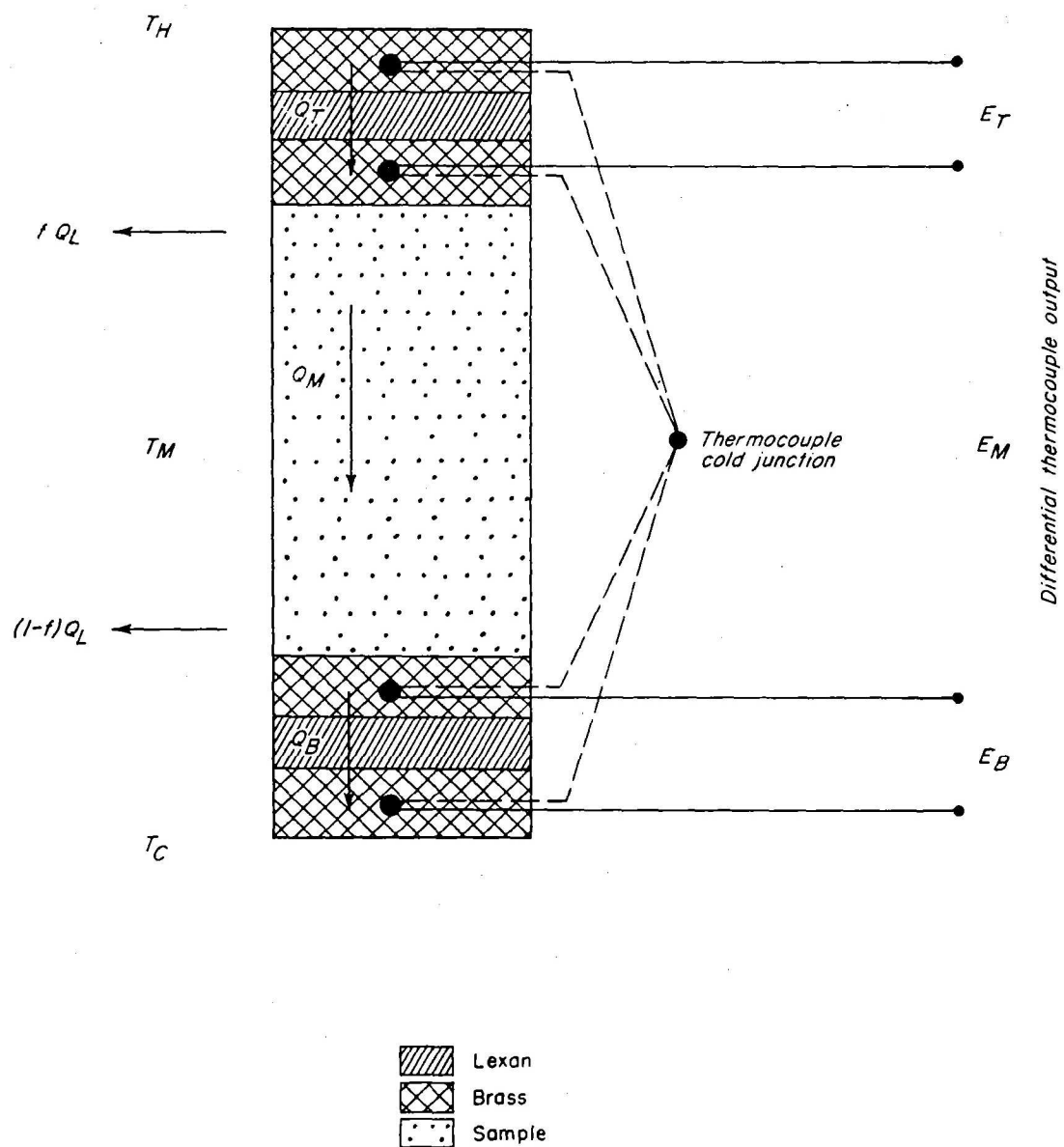


Fig.4 Heat flux in principal segments of divided-bar sample stack.

15

Now $Q = \lambda \Delta T/Z$ and $\Delta T \propto E$ (where ΔT is the temperature drop, E is the thermocouple output, and Z is the thickness of each segment). Additionally since the stack is constructed symmetrically $\lambda_T \approx \lambda_B (= \lambda_L)$ and $z_T \approx z_B (= z_L)$. Equation (8) can therefore be expressed as

$$\frac{z_L}{\lambda_L} \frac{(\lambda_M E_M)}{(z_M)} = E_T - f (E_T - E_B) \quad (9)$$

To proceed with this equation, the factor f must be determined. It can be assumed from considerations of symmetry in Figure 4 that $T_M \approx \frac{1}{2} (T_H + T_C)$. If the insulation is at a temperature T_I the radial heat losses can be expressed as

$$f Q_L \propto \frac{1}{2} (T_H + \frac{1}{2} (T_H + T_C)) - T_I \quad (10a)$$

$$(1 - f) Q_L \propto \frac{1}{2} (T_C + \frac{1}{2} (T_H + T_C)) - T_I \quad (10b)$$

At the beginning of a series of measurements the insulation is at a uniform temperature and usually $T_I \approx T_C$. Adopting this relationship and dividing equation (10a) by (10b) we obtain the result $f = 0.75$. However, during a lengthy series of measurements the insulation heats up; uniformity is lost and lateral temperatures can become matched over the full length of the stack. T_I becomes a complex function of time and space, but, in the limit, a small and constant temperature difference is maintained in each segment. The right hand sides of equations 10a and 10b become identical in magnitude and consequently $f = 0.5$. Values for f will generally vary between these two extremes, but for most purposes we can adopt the average value $f = 0.625$.

The calibration can now be continued with a core of quartz crystal in the sample space. In these circumstances λ_L can be extracted from equation (9) in terms of known or measurable parameters. For LEXAN in the BMR apparatus, equation (9) gives a conductivity $\lambda_L = 0.205 \pm 0.002$ (W.m⁻¹.K⁻¹). This value is adopted for all subsequent work; required values of λ_M can then be extracted from equation (9) when the sample space is occupied by ordinary core.

In summary, with quartz crystal in the sample space, the conductivity of the standards is calculated according to the expression (assuming $f \approx 0.625$ in equation 9).

$$\lambda_L = \frac{(\lambda_M E_M)}{(z_M)} \text{ Qtz} \quad \frac{(8 z_L)}{(3E_T + 5E_B)} \text{ Qtz} \quad (11)$$

This value is then adopted for all subsequent work and the conductivity of ordinary core samples is given by the expression

$$\lambda_M = \frac{(\lambda_L)}{(8 z_L)} \quad \frac{(3E_T + 5E_B)}{(E_M)} z_M \quad (12)$$

These equations were verified by placing a core of silica glass in the sample space. With $\lambda_L = 0.205 \pm 0.002 \text{ (W.m}^{-1} \cdot \text{K}^{-1})$ a value of $1.38 \pm 0.01 \text{ (W.m}^{-1} \cdot \text{K}^{-1})$ was obtained from equation (12) for the conductivity of silica glass. This result compares closely with Ratcliffe's (1959) value of $1.36 \pm 0.01 \text{ (W.m}^{-1} \cdot \text{K}^{-1})$ at 20°C giving an agreement better than 1.5%.

Contact resistance

No allowance has been made in the previous section for the effect of contact resistance within the stack segments. Intuitively it is expected that contact resistance will be very small since all surfaces are polished flat and the stack is kept under an axial pressure of 10 MPa. Significant air gaps should not exist; even so there will always be some remanent contact resistance due to grain plucking (Beck, 1976). The effective conductivity in each segment is further reduced by the presence of the brass discs (used solely to house the thermocouples).

In each segment a total thermal resistance can be defined as

$$R = \frac{z}{\lambda} + r \quad (13)$$

where λ and z are respectively the thermal conductivity and the thickness of the materials within the stack and r contains both the resistance of the brass discs and the contribution from surface contacts. Using this expression, equations (11) and (12) can be restated to give

$$\left(\frac{Z_L}{\lambda_L} + r \right) = \left(\frac{3E_T + 5E_B}{8E_M} \right)_{Qtz} \left(\frac{Z_M}{\lambda_M} + r \right)_{Qtz} \quad (14)$$

and

$$\left(\frac{Z_M}{\lambda_M} + r \right) = \left(\frac{3E_T + 5E_B}{E_M} \right)_{Qtz} \left(\frac{Z_M}{\lambda_M} + r \right)_{Qtz} \left(\frac{E_M}{3E_T + 5E_B} \right) \quad (15)$$

It follows from equation (15) that a straight line will result if values of E_M are plotted against thickness (Z_M) for a suite of samples

$$\frac{3E_T + 5E_B}{E_M}$$

physically identical in other respects. Exact values of r and λ_M can be found by solving for slope and intercept. An example for the BMR apparatus is shown in Figure 5. For soda glass it is found that $\lambda_M = 1.10 \pm 0.01$ W.m.⁻¹.K⁻¹ and $r = 0.0002 \pm 0.00003$ m².K¹.W⁻¹. This value for r is equivalent to 0.3 mm of silica glass; in general it contributes less than 2% to the resistivity of each segment. For most purposes therefore the effect of r can be neglected and thermal conductivities can be determined through equation (12).

CONDUCTIVITY OF FRAGMENTS

Many rocks are of friable nature and it is not possible to place samples under axial pressures in the divided-bar apparatus. Additionally in many instances only drill cuttings are available. If thermal conductivity is to be determined in such circumstances a cell must be used to confine the sample and maintain a precise geometry. A suitable technique has been described by Sass et al. (1971b). Rock fragments are packed into a cell (Fig. 6) and all voids are filled with water (using vacuum). The loaded cell is placed in the sample space of the divided bar and it is then run as a normal core sample. The apparent conductivity (λ_C) is determined and is related to the rock conductivity (λ_R) by the expression

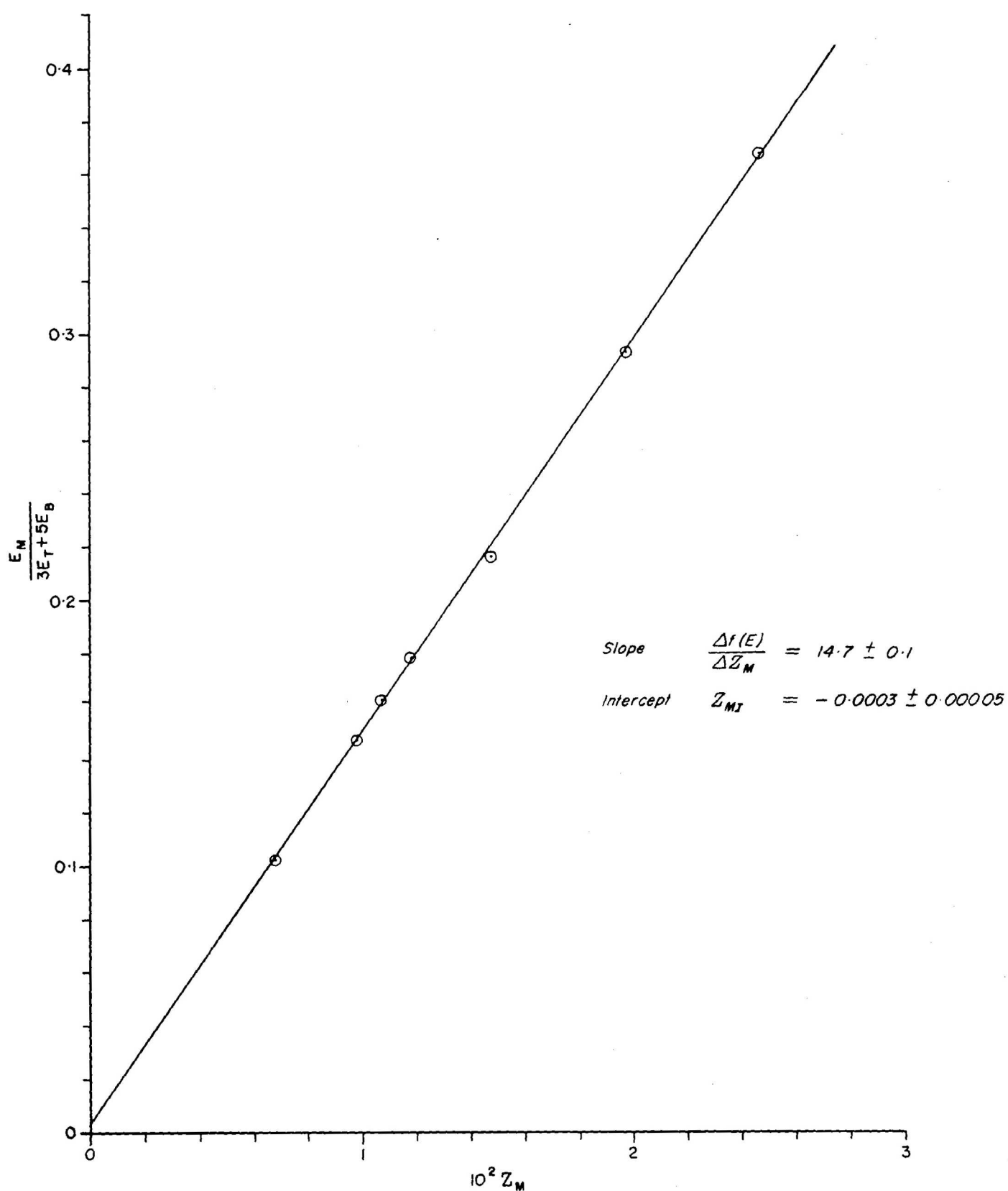


Fig.5 Determination of contact resistance in divided-bar stack segments.

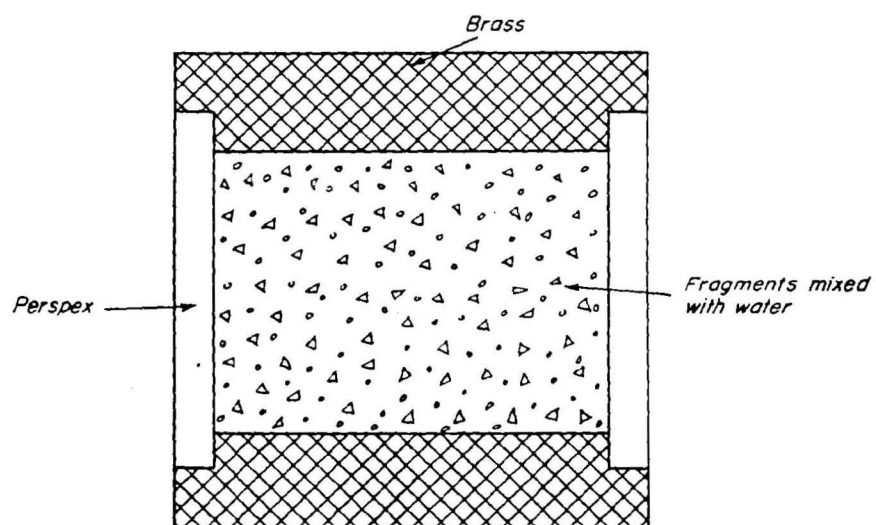


Fig.6 Cell designed to contain core fragments in divided-bar apparatus.

$$\lambda_R = \lambda_W \left[\frac{(D^2)}{(d^2)} \frac{\lambda_C}{\lambda_W} - \frac{(D^2 - d^2)}{(d^2)} \frac{\lambda_P}{\lambda_W} \right] \frac{1-\phi_0}{1-\phi} \quad (16)$$

where d is the inside diameter of the cell, D is the outside diameter, ϕ is the total porosity of the cell, ϕ_0 is the porosity of the original fragments, λ_W is the conductivity of water, and λ_P is the conductivity of the plastic walls of the cell.

Equation (16) is not based on any of the well formulated models of pore/fragment distribution (Woodside & Messmer, 1961); instead a simple geometric mean of volume-weighted conductivities is used as an approximation. Even so, Sass et al. quote an accuracy of $\pm 10\%$ in comparison with solid core. For chips of fused silica the average of 17 determinations was within $\pm 1\%$ of the core value.

The technique was tested in the BMR apparatus using samples of silica glass, soda glass, marble, basalt, granite, and sandstone. The results are shown in Figure 7; they indicate a consistent error of $20 \pm 10\%$. It was observed during these tests that the cell deformed under pressure. The decrease in height was estimated at 3%, but this is insufficient to explain the discrepancies in Figure 7.

The cell technique remains useful because of the good correlations obtained during the tests. Results calculated through equation (16) should, however, be reduced by a factor of 20%.

4. CALCULATIONS OF HEAT FLOW

Heat flow is determined simply from the product of the thermal gradient and the thermal conductivity (equation 1). However, there are sampling errors in both parameters. Thermal gradients are calculated from discrete measurements of temperature at depth intervals usually greater than 5 m. Even if core is available there would rarely be more than one measurement of thermal conductivity in the same interval. In highly variable sedimentary strata it may not be possible to choose a core sample representative of the whole interval; the accuracy of heat flow determinations would then depend on the uniformity of the lithology. In practice, heat flow is determined for several intervals and the results are averaged to give estimates of error. However, since all conductivity samples must be machined before they are placed in the divided-bar apparatus, there may be a bias toward well consolidated core. Computed results would then be too large.

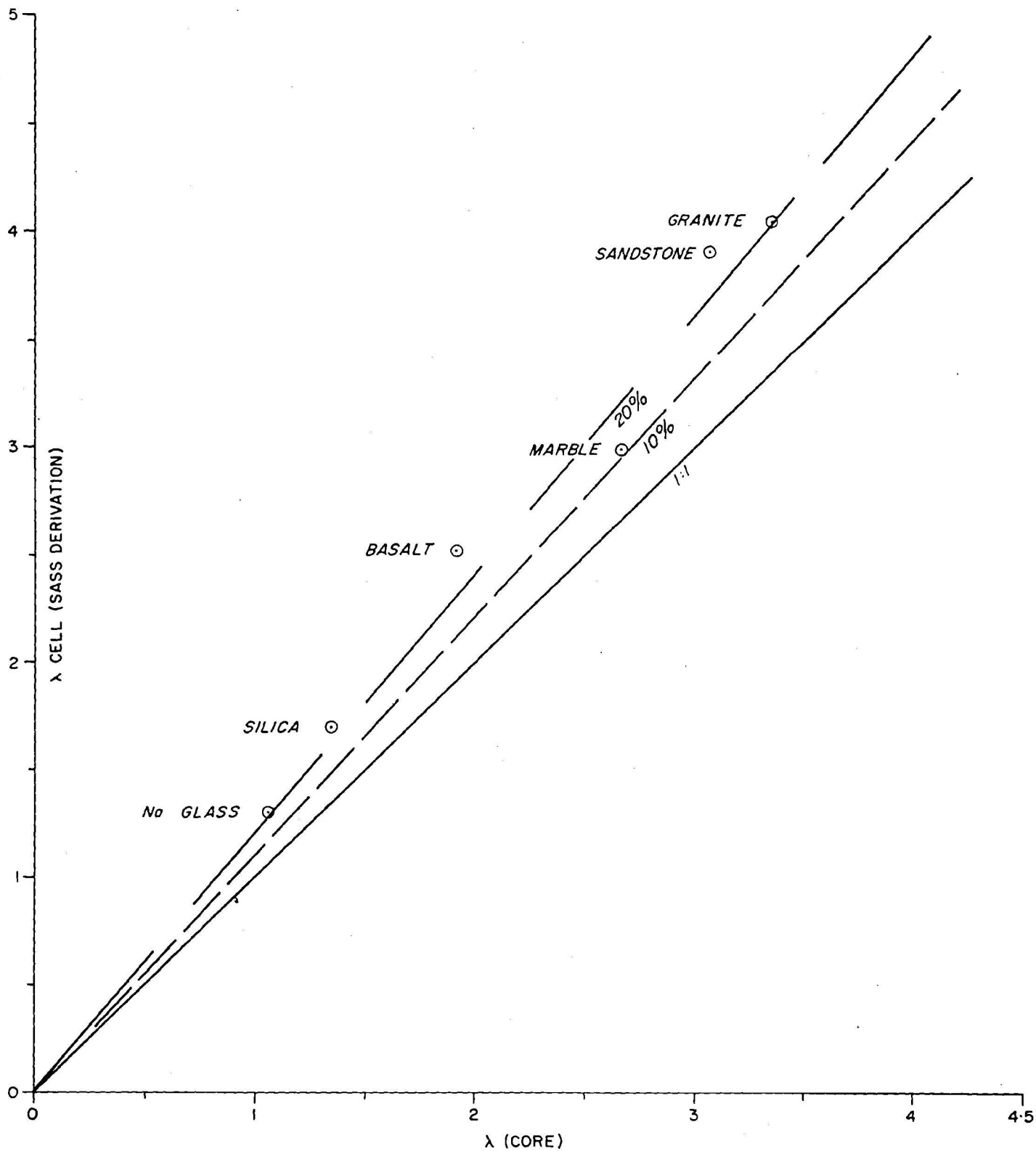


Fig.7 Comparison of conductivity values determined using (1) solid core and (2) fragments.

If borehole stratigraphy is well known, heat flow can be determined from estimates of interval resistivity (Bullard, 1939). Assuming that heat flow is constant through all intervals, the temperature at any depth can be expressed as

$$T_Z = T_0 + Q \sum_i (D_i / \lambda_i) \quad (17)$$

where D_i is the interval resistivity; D and λ_i are the thickness and

conductivity of each section of uniform lithology and the depth $Z = \sum_i D_i$. Conductivities can be assigned to each rock type and a value of Q can be obtained by plotting $\sum_i D_i / \lambda_i$ against values of T . Conductivities must be determined for all types of core, and bias can therefore be avoided. Additionally, correlation coefficients obtained from the plot can be used for an estimate of error.

The constant T_0 in equation (17) can be obtained by extrapolating to the surface from temperatures observed at depths greater than 30 m. Howard & Sass (1964) have shown that values of T_0 obtained in this manner are, on average, 3°C greater than the mean annual air temperature in each location. Discrepancies can be expected from variations in the Earth's albedo but, in general, values of T_0 can be reasonably estimated from Figure 8. The Bullard reduction can therefore proceed even if near-surface temperature gradients are perturbed by groundwater movements or by surface weathering.

The techniques used for calculating Q are shown in Figures 9 and 10. The data were obtained from a stratigraphic hole drilled through limestone in the Canberra 1:250 000 Sheet area (BMR reg. no. CAN 145, lat. 35.30° , long. 149.15°). Although there is curvature in the geothermal gradient there are corresponding changes in thermal conductivity; computed values of Q are consequently substantially constant. At depths greater than 100 m the Bullard plot (equation 17) shows extremely good correlation since there are no rapid changes in lithology and all conductivities are well determined. Taking the average from both techniques we find a value $Q = 72.9 \pm 2.7 \text{ mW.m}^{-2}$. This result is generally consistent with results previously reported for the Canberra region: $86.1 \pm 1.6 \text{ mW.m}^{-2}$ at Mount Stromlo and $100.3 \pm 3.4 \text{ mW.m}^{-2}$ at Captains Flat (Sass et al., 1976).

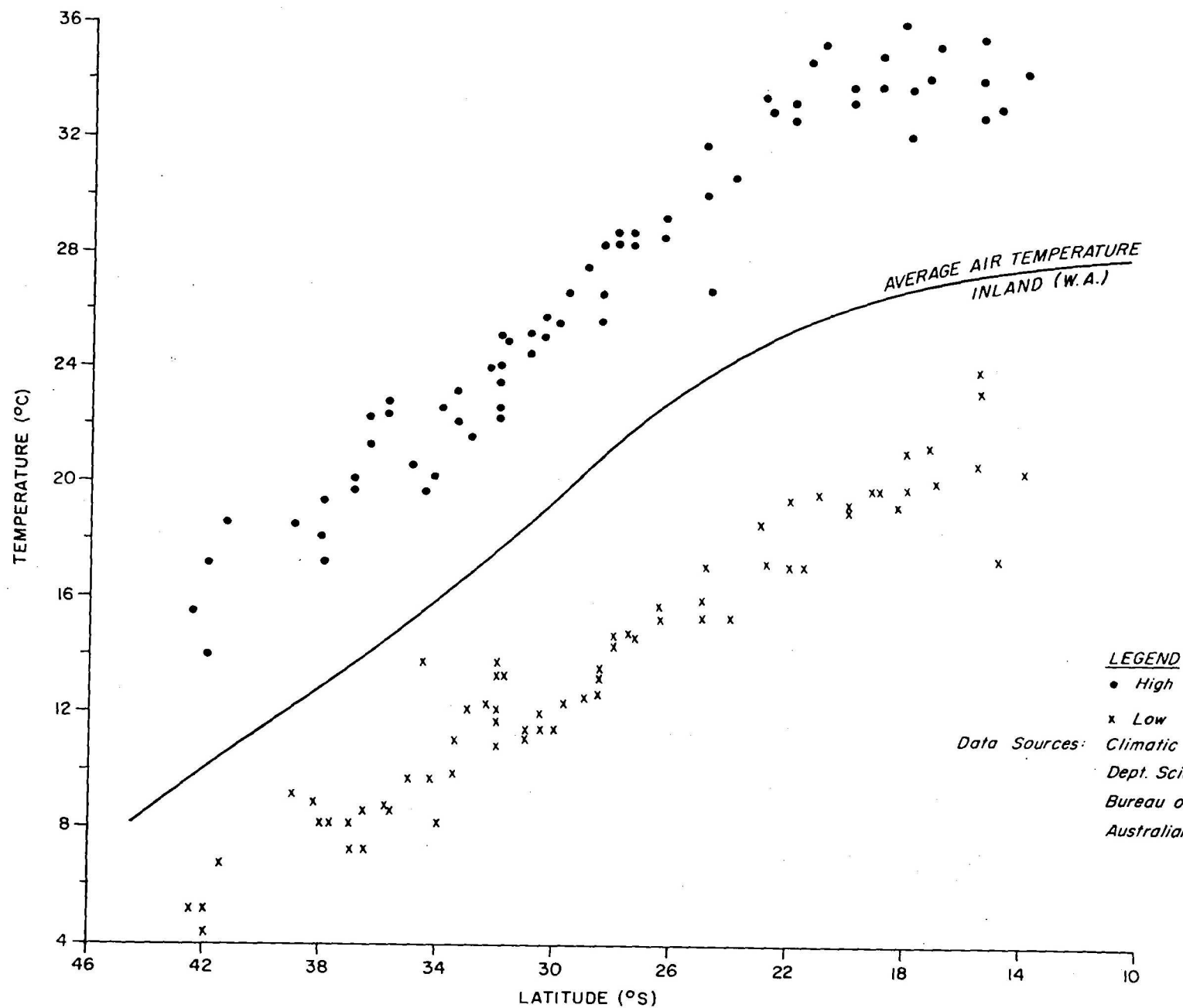


Fig. 8 Mean annual air temperature as a function of latitude.

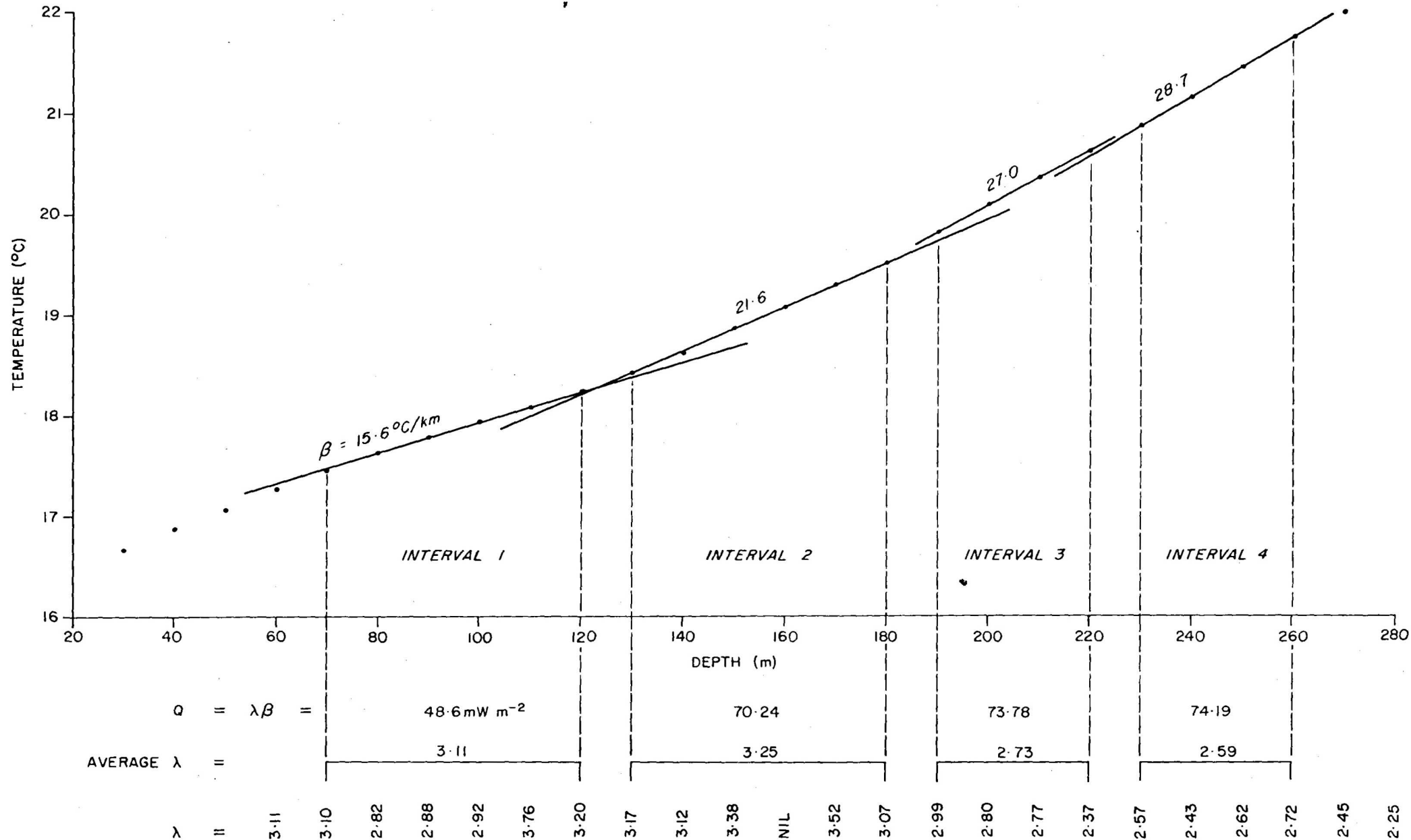


Fig.9 Temperature/depth profile for borehole CAN 145. Determinations of heat flow from linear segments.

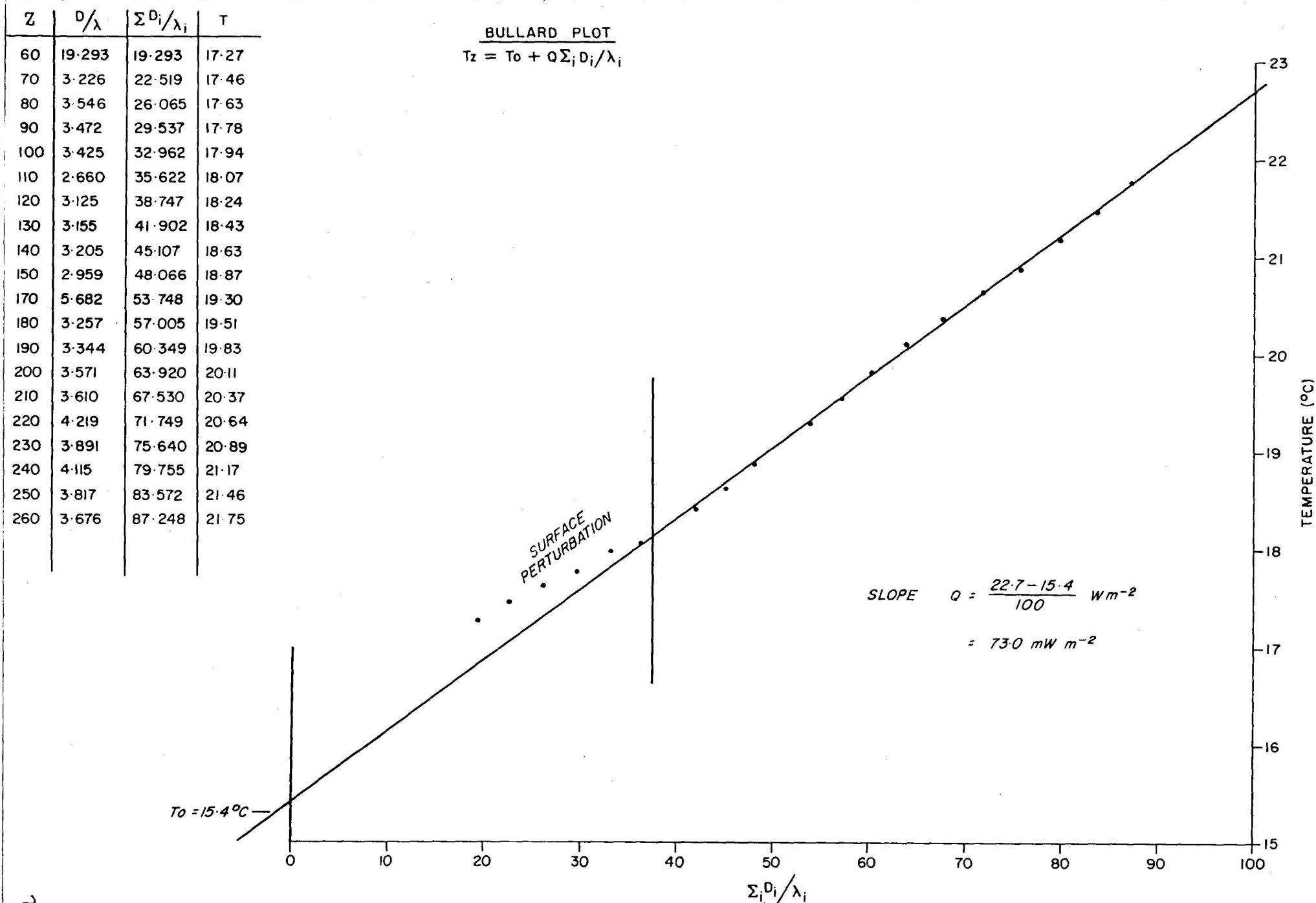


Fig.10 Bullard reduction of data presented in Fig.9. Determination of heat flow.

5. ACKNOWLEDGEMENTS

The divided-bar apparatus was constructed to exacting specifications by R.I. Eaton of the BMR Rock Measurements group. In addition to design and specification of all the major components this group was also responsible for initial development of data reduction techniques. The Wheatstone bridge was constructed by B. Liu and S. Scherl in the BMR Design and Development laboratories.

6. REFERENCES

- AULD, M.J., 1948 - Temperature gradients for convection in well models. J. Appl. Phys., 19, 218.
- BECK, A.E., 1959 - A steady state method for the rapid measurement of the thermal conductivity of rocks. J. Sci. Instr., 34, 186.
- BECK, A.E., 1976 - An improved method of computing the thermal conductivity of fluid-filled sedimentary rocks. Geophys., 41, 133.
- BIRCH, F., 1950 - Flow of heat in the Front Range, Colorado. Bull. Geol. Soc. Am., 61, 567.
- BULLARD, E.C., 1939 - Heat flow in South Africa. Proc. Roy. Soc. London, A173, 474.
- BULLARD, E.C., 1947 - Time necessary for a borehole to attain temperature equilibrium. Monthly Notices Roy. Astr. Soc., Geophys. Suppl., 5, 125.
- CARSLAW, H.S., & JAEGER, J.C., 1959 - Conduction of Heat in Solids, second edition, Oxford University Press, London.
- DIMENT, W.H., 1967 - Thermal regime of a large diameter borehole; instability of water column and comparison of air and water filled conditions. Geophys., 23, 720.

- ELDER, J.W., 1965 - Physical processes in geothermal areas, in Terrestrial Heat Flow, A.G.U. monograph 8.
- GRETENER, P.E., 1967 - On the thermal instability of large diameter wells - an observational report. Geophys., 23, 727.
- HALES, A.L., 1937 - Convection currents in geysers. Monthly Notices Royal Astr. Soc., Geophys. Suppl., 4, 122.
- HORTON, C.W., & ROGERS, F.T., 1945 - Convection currents in a porous medium. J. Appl. Phys., 16, 367.
- HOWARD, L.E., & SASS, J.H., 1964 - Terrestrial heat flow in Australia, J. Geophys. Res., 69, 1617.
- KRIGE, L.J., 1939 - Borehole temperatures in the Transvaal and Orange Free State. Proc. Roy. Soc., A173, 450.
- LAPWOOD, E.R., 1948 - Convection of a fluid in a porous medium, Proc. Cambridge Phil. Soc., 44, 508.
- RATCLIFFE, E.H., 1959 - Thermal conductivities of fused and crystalline quartz. Brit. J. Appl. Phys., 10, 22.
- SASS, J.H., LACHENBRUCH, A.H., MUNROE, R.J., GREEN, G.W., & MOSES, T.H., 1971a- Heat flow in the western United States. J. Geophys. Res., 76 6376.
- SASS, J.H., LACHENBRUCH, A.H., & MUNROE, R.J., 1971b - Thermal conductivity of rocks from measurements on fragments and its application to heat flow determinations. J. Geophys. Res., 76, 3391.
- SASS, J.H., JAEGER, J.C., & MUNROE, R.J., 1976 - Heat flow and near-surface radioactivity in the Australian continental crust. USGS Open-File Report 76/250.

TUCKER, G.B., 1975 - Climate: is Australia's changing? Search, 6, 323.

WOODSIDE, W., & MESSMER, J.H., 1961 - Thermal conductivity of porous media.
J. Appl. Phys., 32, 1688.

Captions

- Fig. 1 Schematic for eliminating lead resistance in Wheatstone bridge circuit used with a down-hole thermistor probe.
- Fig. 2 Secular perturbation of temperature gradient (step function of 5°C at surface).
- Fig. 3 Principal components in divided-bar thermal-conductivity apparatus.
- Fig. 4 Heat flux in principal segments of divided-bar sample stack.
- Fig. 5 Determination of contact resistance in divided-bar stack segments.
- Fig. 6 Cell designed to contain core fragments in divided-bar apparatus.
- Fig. 7 Comparison of conductivity values determined using (1) solid core and (2) fragments.
- Fig. 8 Mean annual air temperature as a function of latitude.
- Fig. 9 Temperature/depth profile for borehole CAN 145. Determinations of heat flow from linear segments.
- Fig. 10 Bullard reduction of data presented in Fig. 9. Determination of heat flow.